Observation of Electron Trapping and Phase-Area Displacement in the Interaction between an Electron Beam and Two Counterpropagating Laser Beams

R. Z. Olshan, A. Gover, S. Ruschin, and H. Kleinman
Department of Physical Electronics, Faculty of Engineering, Tel-Aviv University, Israel
(Received 30 September 1986)

We report the observation of synchronous energy exchange between nonrelativistic electrons and the ponderomotive (beat) force of two counterpropagating, intense, pulsed CO_2 laser beams, operating at different frequencies in a stimulated Compton-scattering scheme. The interaction takes place in the nonlinear (trapping) regime, and its physics is the same as in laser accelerators and efficiency-enhanced free-electron lasers with long wigglers. Two different mechanisms of enhanced energy transfer were observed—electron trapping and phase-area displacement.

PACS numbers: 42.55.Tb, 29.15.−n, 41.70.+t, 52.75.Ms

A single electron cannot exchange energy with a single electromagnetic (EM)-wave photon in free space, because conservation of both energy and momentum cannot be satisfied simultaneously. Consequently, the lowest-order radiative-interaction process in free space involves two photons. The most basic process of this kind is Compton scattering.

A *stimulated* Compton-scattering effect was predicted in 1933 by Kapitza and Dirac.[1] In their configuration, two counterpropagating EM waves of equal frequency form a standing wave. If an electron, propagating transversely to the waves, scatters a photon from one traveling wave to the other, it obtains transverse momentum $2\hbar\omega/c$, and therefore may be deflected by an angle of $(2\hbar\omega/c)/\gamma mv$. As the EM wave intensities are increased, the deflection process can be described as electron diffraction by a spatially periodic ponderomotive potential "grating," which is generated by the beat of the two EM waves.[2]

If the free electron is propagating in a counter direction to an incoming EM wave, the scattered Compton radiation exhibits a Doppler shift. In the case of backscattering, the scattered (signal) wave frequency ω_s is related to the incoming (wiggler) wave frequency ω_w by

$$\omega_s/\omega_w=(1+\beta_z)/(1-\beta_z), \tag{1}$$

where $\beta_z=v_z/c$ is the electron axial velocity, and the small quantum recoil effect was neglected. At relativistic electron velocities the Doppler shift associated with (1) may be appreciable, and this can be utilized to advantage in stimulated Compton-scattering free-electron lasers (FEL), where the signal wave is amplified by the stimulated Compton-scattering process.[3] Similar stimulated emission or absorption may also be obtained with a periodic magnetostatic wiggler field, as employed in magnetic bremsstrahlung FEL[4] and laser accelerators.[5]

In order to observe an appreciable interaction effect between the electrons and the traveling beat wave, the electron velocity must be synchronized with the beat-wave phase velocity $v_r=(\omega_s-\omega_w)/(k_s+k_w)$ (for a static wiggler $\omega_w=0$). The relative velocity between the electron and the wave can be scanned by application of an axial electric field. In the nonlinear regime, where deep ponderomotive potential wells (traps) form, two different physical situations may occur: (1) electrons inserted into the interaction region are within the phase-space area of initially synchronous traps [trapping, see Fig. 1(a)] and (2) the opposite case of no initial trapping [Fig. 1(b)]. If the axial field E and other interaction parameters are uniform along the entire interaction length, the initially trapped electrons occupy closed trajectories inside the trap area, and remain trapped despite the accelerating field. In both cases the initially untrapped electrons accelerate or decelerate freely, following open phase-space trajectories. Transitions between trapped and untrapped electron trajectories are possible only if the interaction parameters are changed nonadiabatically in either the axial or time dimension, or if the electron is displaced transversely across the optical beams.

The phase-space diagram of Fig. 1(a) depicts partial

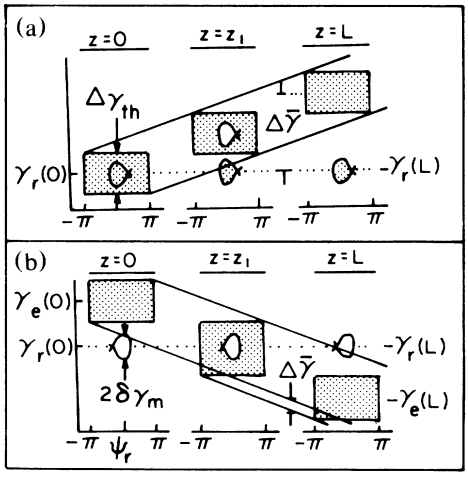

FIG. 1. Phase-space diagrams for electron energy extraction: (a) electron trapping; (b) phase-area displacement.

initial trapping by a constant-velocity ponderomotive potential wave in the presence of an accelerating electric field.[6] The trapped electrons do not accelerate, and consequently produce enhanced stimulated Compton-scattering radiation into the signal field. Figure 1(b) depicts an alternative mechanism of radiative energy extraction from *untrapped* electrons in the presence of a *decelerating* field. This "phase-area displacement" (PAD) mechanism[7,8] causes enhanced signal radiation when the entire electron beam is decelerated through the synchronism condition. Note that under the same direction of dc field the trapped-electron and the PAD mechanisms would result in energy exchange with the radiation fields in opposite directions.

The FEL efficiency-enhancement scheme of a tapered-period static wiggler with a decelerating beat wave has essentially the same physics as the axial electric-field scheme.[7] Such FEL were recently demonstrated to operate with remarkable efficiencies.[9] Laser accelerators with inverse tapering have been considered,[5] and PAD-FEL accelerator schemes have been proposed,[7,8] but neither has yet been tried. A more direct experimental tool for the study of electron interactions with intense radiation fields—the stimulated Compton-scattering scheme—has not yet been exploited, although state-of-the-art high-intensity lasers make it possible to study these interaction effects in both the linear and nonlinear regimes. There have been some attempts to study stimulated Compton scattering in the Kapitza-Dirac configuration, utilizing the high-intensity standing wave field inside the cavity of a ruby laser.[10]

This Letter describes a novel scheme for investigating nonlinear-regime stimulated Compton scattering in the traveling beat wave of two counterpropagating laser beams. An experiment with similar features was reported recently by Martin *et al.*[11] In that experiment electrons were accelerated by a plasma wave excited by the beat of two CO_2 laser beams, whereas in our experiment, we deal directly with the stimulated Compton-scattering interaction between the electromagnetic waves and electrons.

The experiment concept as depicted in Fig. 2 with the baseline parameters listed in Table I was described in detail by Olshan *et al.*[12] Two transversely excited atmospheric CO_2 lasers produced the 9.3-μm signal wave and the 10.6-μm wiggler wave, both of which were operated in single longitudinal and transverse cavity modes. Their

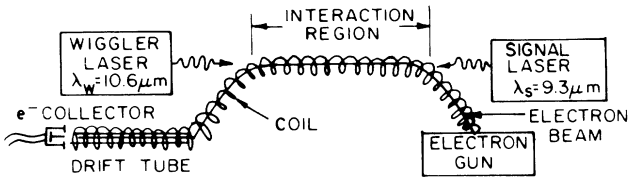

FIG. 2. Experimental conceptual diagram.

100-ns-duration pulses were synchronized to arrive simultaneously at the interaction region during the 10-μs pulse of the electron beam. The ~1-keV electron-beam voltage was matched to the synchronism condition (1) either at the entrance to the interaction region for setting trapping conditions [Fig. 1(a)], or within the interaction region for PAD [Fig. 1(b)]. The electron beam energy spread was $\Delta E_{th} \simeq 4$ eV, with a grid-controlled current of 10–50 μA.

An axial electric force was exerted along the interaction length by employment of the Ohmic potential drop developed along a copper coil when a 1-ms, 500-A current pulse is applied to it. Accelerating or decelerating fields were achieved by a change of direction of the current. The coil current also provided an axial magnetic field which bent the electron-beam and guided it along the interaction region.

Both retarding-potential and time-of-flight electron-energy analysis techniques were employed. In the first method a retarding-potential electrode is placed in front of a Faraday-cup collector, and is biased to set partial electron-beam reflection conditions (V_r=0–7 V). In case of positive transfer of energy from the radiation field to the electrons, a pulse of the excess electrons, which surpass the retarding potential barrier, would arrive at the collector during the laser's pulse period. In case of negative energy transfer, a current-deficiency pulse would be measured. In the time-of-flight technique the tube is biased to a low voltage (V_{dt}=10 V), so that electrons of different velocities, and correspondingly different drift times, produce a time-dispersed current pulse which folds in itself the electron energy spectrum after the interaction.

The electron current pulse and the laser pulses were recorded by three separate channels of high-speed digital transient recorders. The data were stored by an on-line computer for subsequent reduction, analysis, and interpretation.

The basic theory of electron trapping and PAD

TABLE I. Experiment parameters.

Signal power	0.25 MW
Wiggler power	0.25 MW
Signal wavelength	9.261 μm
Wiggler wavelength	10.59 μm
Optical beam waists (w_0)	1.77 mm
Coil current	0.5 kA
Energy spread (FWHM)	3 eV
Interaction length	0.6 m
Electron current	10 μA
Electron velocity	2.0×10^7 m/sec
Axial electric field	65 V/m
Resonance energy	1.153 keV
Ponderomotive field	369.7 V/m
Trap depth	1.409 eV
Resonant phase ψ_r	0.2 rad

efficiency-enhancement schemes in magnetic bremsstrahlung FEL's is given in Refs. 7 and 8. The electron axial motion is governed by the longitudinal force equation

$$d(\gamma m v_z)/dt = -eE_{ac} - eE_p \cos\psi(z,t), \quad (2)$$

where E_{ac} is an externally applied axial accelerating or decelerating dc electric field, and E_p is the ponderomotive field amplitude, which for the case of an EM wiggler is given by[13]

$$E_p = \frac{e(\mu_0/\varepsilon_0)^{1/2}}{\gamma_r mc^2}(\lambda_s + \lambda_w)\,|\hat{\mathbf{e}}_s \cdot \hat{\mathbf{e}}_w^*|\,\frac{(P_w P_s)^{1/2}}{\pi w_{0s} w_{0w}}, \quad (3)$$

where $\hat{\mathbf{e}}_i$, P_i, w_{0i} $(i = w,s)$ are the polarization unit vectors, the powers, and beam waists of the wiggler and signal waves, respectively. The phase of the electron relative to the ponderomotive wave is $\psi = (\omega_s - \omega_w)t - (k_s + k_w)z$.

First integration of the pendulum-type equation (2) results in closed (trapped) or open electron phase-space orbits inside or outside the separatrix, respectively. The separatrix function (shown in Fig. 1) is characterized by two parameters: the resonant phase ψ_r, and the zero-field half-width (HW) of the trap $\delta\gamma_t^0$ given by[13]

$$\psi_r = \arcsin(E_{ac}/E_p), \quad (4)$$

$$\delta\gamma_t^0 = [4e\beta^2\gamma^3 E_p/(k_s + k_w)mc^2]^{1/2}. \quad (5)$$

For $\psi_r = 0$, the separatrix function is simply $\delta\gamma = \delta\gamma_t^0 \times |\cos(\psi/2)|$. For $\psi_r \neq 0$, it is given by another periodic function with reduced phase-space dimensions of the trap[7,8]: $\delta\gamma_m < \delta\gamma_t^0$, $\Delta\psi < 2\pi$ (see Fig. 1). With uniform acceleration along the interaction region, electrons that are trapped inside the interaction region remain trapped to the end [Fig. 1(a)], and are displaced by average energy $\Delta\bar{\gamma}$, relative to the untrapped ones, where

$$\Delta\bar{\gamma} = eE_{ac}L/mc^2, \quad (6)$$

and L is the interaction length. For a warm electron beam, $\Delta\gamma_{th} \gg 2\delta\gamma_m$, the trapping efficiency will be $A_t/2\pi\Delta\gamma_{th}$, where A_t is the trap area ($A_t \simeq 8\delta\gamma_t^0$ for $\psi_r \ll 1$).

If the decelerated or accelerated electron-beam synchronizes with the beat wave within (as opposed to at the start of) the interaction region [Fig. 1(b)], the beam will exchange average energy $\Delta\bar{\gamma}$ with the radiation field by the PAD mechanism. $\Delta\bar{\gamma}$ may be calculated by integration along phase-space paths of the electrons. For $\psi_r \ll 1$, with neglect of edge effects, an approximate expression is derived[7,8]:

$$\Delta\bar{\gamma} = A_t/2\pi = 4\delta\gamma_t^0/\pi. \quad (7)$$

Even if the initial electron-beam energy spread is large, this average energy transfer will affect all the electrons, since they all pass through synchronism with the beat wave.

Initial experiments were carried out with a decelerating axial electric field employing the parameters of Table I and the system shown in Fig. 2 operating in the retarding-potential mode (with the drift tube eliminated). The retarding electrode was set to $V_r < 1$ V to reflect most of the current. The initial energy of the beam V_i was scanned to vary the position of synchronism along the interaction region. The signal intensity, which is proportional to the number of electrons acquiring energy from the radiation field, exhibited a resonance curve as a function of V_i as shown in Fig. 3. The peak of the curve corresponds to beam energy at synchronism condition with the beat wave in the center of the interaction region, where the laser fields were most intense. Its width corresponds to the potential drop along the interaction region ($E_{ac}L = 40$ V). These findings correspond well with the results expected for a PAD energy exchange at those characteristic resonance conditions. However, with this interpretation we explain the measured excess electron current pulses as a result of PAD-interaction-induced energy spread. The expected average *net* effect of PAD deceleration was supposedly less dominant in these experimental conditions.

Because the retarding-potential method does not give the electron energy spectrum in a single pulse, and because the energy exchange in the interaction turned out to be smaller than the initial energy spread, it was hard to resolve by this method the direction of *net* energy transfer between the beam and the radiation field. Indeed, signals with both current excess and deficiency were measured at various V_r values with either of the coil-current polarities. In order to resolve this problem and to identify distinctly the occurrence and conditions for trapped-electron and PAD interaction effects, we resorted to employment of the time-of-flight energy-analysis technique. The experimental scheme of Fig. 2 was operated with basically the same parameters of Table I but with $\lambda_s = 9.25$ μm, $\lambda_w = 10.59$ μm, $E_{ac} = 42$ V/m (accelerating field), and drift-tube voltage $V_{dt} = 10$ V. Figure 4 shows the measured collector current signal

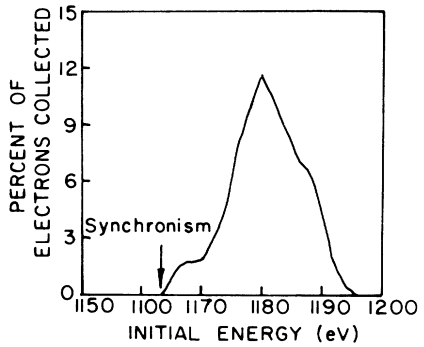

FIG. 3. Collector current signal vs initial electron energy. The arrow marks synchronism at the interaction-region entrance.

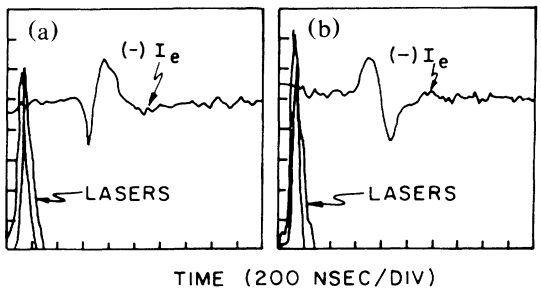

FIG. 4. Collector current signals corresponding to electrons (a) accelerated and (b) decelerated by the radiation field. (a) $V_i = 1155$ V, PAD conditions; (b) $V_i = 1165$ V, trapping conditions.

for two values of initial voltage of the beam: (a) $V_i = 1155$ V corresponding to synchronism near the center of the interaction region, and (b) $V_i = 1165$ V corresponding to synchronism precisely at the entrance to the interaction region. In both cases the signals appear with a transit-time delay (~ 0.6 μs) relative to the coincident laser pulses, but the signals are temporally inverted relative to each other, indicating opposing energy-transfer directions. The oscillogram of Fig. 4(a) with an initially negative (excess current) signal followed by a positive (charge depletion) signal, indicates net electron acceleration by the laser pulses, as expected for a PAD energy-exchange process. Conversely, the signal of Fig. 4(b) indicates electron deceleration and thus energy transfer to the radiation field in agreement with predictions for electron trapping.

The experimental data demonstrate that both trapping and PAD mechanisms of energy exchange were observed in the stimulated Compton-scattering scheme at the conditions predicted by theory. Because of the large initial beam-energy spread, which was apparently larger than the net energy transfer, the positive and negative parts of the signals were not completely resolved in time, and it was hard to determine the exact amount of energy exchanged with the radiation field in either mechanism. However, simulation of the drift-tube transport dynamics with the known initial electron energy distribution (measured by scanning of the retarding potential) and with assumptions of energy transfer $\Delta\bar{E} \simeq +1.5$ eV and $\Delta\bar{E} \simeq -2.0$ eV, fitted reasonably well with the wave forms of Figs. 4(a) and 4(b), respectively. The +1.5-eV PAD energy transfer compares well with the $\bar{E} \simeq +1.6$ eV predicted from Eq. (7). The −2.0-eV energy transfer corresponds to electron detrapping after 5 cm, possibly a result of nonuniformities in the dc fields, lateral deviations in the overlapping of the beams, or the finite coherence of the laser beams.

The successful demonstration of energy exchange by nonlinear-regime Compton scattering in the present experiment makes way for further fundamental-interaction and FEL-related studies in a small-scale laboratory system. Further experiments to be carried out with this system will provide opportunities to study important interaction aspects of phase-area displacement and trapping mechanisms, for example, effects of nonadiabatic changes in the interaction parameters and incoherence of the wiggler and signal waves. The large number of wiggler periods (5×10^4) and trap synchrotron oscillations (~ 40) puts this lasers' beat experiment in the interesting regime of very-long-wiggler FEL's and laser accelerators, where studies of phase-space evolution has important fundamental and applied research implications.

This work was supported initially by the United States Air Force through Grant No. AFOSR 82-0289 and subsequently by endowments from the Kranzberg Institute and Israeli Universities funding committee. A. Friedman, I. Katz, A. Eichenbaum, B. Cohen, P. Yogev, and B. Lissak made important contributions to the experiment construction. We thank C. Brau and P. Morton for suggesting the PAD scheme as an interpretation of our initial experimental results.

[1]P. L. Kapitza and P. A. M. Dirac, Proc. Cambridge Philos. Soc. **29**, 197 (1933).

[2]M. V. Fedorov, Prog. Quantum Electron. **7**, 73 (1981).

[3]R. H. Pantell, G. Soncini, and H. E. Puthoff, IEEE J. Quantum Electron. **4**, 905 (1968).

[4]D. A. G. Deacon *et al.*, Phys. Rev. Lett. **38**, 892 (1977).

[5]E. D. Courant, C. Pellegrini, and W. Zakowicz, Phys. Rev. A **32**, 2813 (1985).

[6]A. Gover, C. M. Tang, and P. Sprangle, J. Appl. Phys. **53**, 124 (1982).

[7]N. M. Kroll, P. Morton, and M. N. Rosenbluth, IEEE J. Quantum Electron. **17**, 1436 (1981).

[8]M. N. Rosenbluth, B. N. Moore, and H. V. Wong, IEEE J. Quantum Electron. **21**, 1026 (1985).

[9]C. A. Brau, IEEE J. Quantum Electron. **21**, 824 (1985); T. J. Orzechowski *et al.*, IEEE J. Quantum Electron. **21**, 831 (1985).

[10]L. S. Bartell, H. Bradford, and R. R. Roskov, Phys. Rev. Lett. **14**, 851 (1965).

[11]F. Martin *et al.*, Bull. Am. Phys. Soc. **30**, 1613 (1985).

[12]R. Z. Olshan *et al.*, Nucl. Instrum. Methods Phys. Res., Sect. A **250**, 253 (1986).

[13]R. Z. Olshan, Ph.D. dissertation, Tel-Aviv University, 1986 (unpublished).